Quantum Information and Computation, Vol. 3, No. 3 (2003) 265–279

INFORMATION THEORETIC ASPECTS IN PONDEROMOTIVE SYSTEMS

S. GIANNINI, S. MANCINI and P. TOMBESI

INFM, Dipartimento di Fisica, Università di Camerino, I-62032 Camerino, Italy

Received February 5, 2003
Revised May 12, 2003

We show the possibility to entangle radiation modes through a simple reflection on a moving mirror. The model of an optical cavity having a movable end mirror, and supporting different modes is employed. The mechanical motion of the mirror mediates information between the modes leading to an effective mode-mode interaction. We characterize the modes' entanglement on the basis of recent separability criteria. The effect of the thermal noise associate to the mirror's motion is accounted for. Then, we evaluate the performances of such *ponderomotive entanglement* in possible applications like teleportation and telecloning.

Keywords: mechanical effects of light, entanglement, quantum teleportation

Communicated by: S Braunstein & C Fuchs

1. Introduction

Ponderomotive systems in optics are physical systems where the electromagnetic pressure force gives rise to relevant effects. The optomechanical coupling between a movable mirror and a radiation field, is realized in such systems when the field is reflected by the moving mirror. This coupling was introduced in the context of quantum limited measurements [1] and then used in interferometric gravitational-wave detection [2] as well as in atomic force microscope [3]. Since then, a wide literature has been devoted to such a coupling. In particular, it has been shown that it may lead to nonclassical states of both the radiation field [4, 5], and the motion of the mirror [6]. The interest about ponderomotive systems also relies on the possibility to investigate, with them, the tricky borderline between the quantum and the classical world [7, 8]. Moreover, recent technical progresses have made this area experimentally accessible [9, 10].

The appearance of quantum effects in ponderomotive systems, paves the way to use them also for quantum information purposes [11]. These require as main ingredient the entanglement [12, 13]. Furthermore, information processing, in the quantum optical framework, can be implemented when applied to continuous quadratures of electromagnetic modes [14]. Then, the use of a ponderomotive meter for continuous variable entanglement purification has been investigated in Ref.[15]. Furthermore, the possibility to obtain quantum correlated quadratures of the field reflected by a movable mirror has been proposed in Refs. [16, 17]. Here,

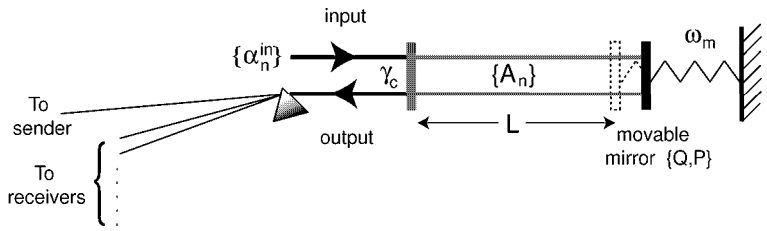

Fig. 1. A possible scheme implementing the studied ponderomotive system.

following the line sketched in Ref.[16], we study a ponderomotive system, namely a radiation field reflected by an oscillating mirror, from the quantum information perspective. In particular, we shall show that the mechanical motion of the mirror mediates information between the field modes leading to an effective mode-mode interaction. Then we shall characterize the modes' entanglement on the basis of recent criteria [8, 18, 19], and we shall evaluate the performances of such ponderomotive entanglement in possible applications like teleportation [20, 21] and telecloning [22]. In our analysis we shall also account for the effect of the thermal noise associate to the mirror's motion. Then, it will become clear the importance of such systems from both foundational and applicative aspects.

The structure of the paper is the following. In Section II, we introduce a multimode ponderomotive model. In Section III, we consider the outgoing fields and their quantum correlations. Then, in Section IV, we study some possible applications. Finally, Section V is for concluding remarks.

2. A ponderomotive system

The model we are going to consider is schematically depicted in Fig.1. It consists of a linear cavity, with an oscillating end mirror, plunged in a thermal reservoir at the equilibrium temperature T. This completely reflecting mirror, with mass m, can move back and forth along the cavity axes. When the cavity is empty the moving mirror undergoes harmonic oscillations at frequency ω_m, damped at rate γ_m by the coupling to the external bath. In presence of a radiation field, the cavity length varies under the action of the radiation pressure force, which causes the instantaneous displacement of the mirror.

The resonant frequencies of the cavity are calculated at the equilibrium position of the oscillating mirror, resulting

$$\omega_{cn} = \frac{\pi\, c}{L}\,\tilde{n}\,, \tag{1}$$

where $\tilde{n}$ is an arbitrary integer number corresponding to the index n, c is the speed of light, and L is the equilibrium cavity length. We consider the possibility to have several input fields at frequencies $\omega_{0\,n} \sim \omega_{c\,n}$ driving the corresponding cavity modes. In the adiabatic limit in which the mirror frequency is much smaller than the cavity free spectral range $c/(2L)$ we can focus only on the driven cavity modes, obtaining the following Hamiltonian

$$H_{tot} \;=\; H_{free} + H_{drive} + H_{int}\,, \tag{2}$$

$$H_{free} = \hbar \sum_n \omega_{c\,n} A_n^\dagger A_n + \frac{P^2}{2m} + \frac{1}{2} m \omega_m^2 Q^2 \,, \tag{3}$$

$$H_{drive} = i\hbar\sqrt{\gamma_c} \sum_n \left(\alpha_n^{in} e^{-i\omega_{0\,n} t} A_n^\dagger - \alpha_n^{in\,*} e^{i\omega_{0\,n} t} A_n \right) \,, \tag{4}$$

$$H_{int} = -\hbar \sum_n \frac{\omega_{c\,n}}{L} A_n^\dagger A_n Q \,, \tag{5}$$

where the sum must be intended over the driven modes. H_{free} is the Hamiltonian for the free motion of the mechanical oscillator (moving mirror) having position Q and momentum P, and of the cavity modes characterized by the ladder operators A_n , $A_n^\dagger$. Here we are considering a multimode radiation model, focusing on the longitudinal modes, differentely from Ref.[17] where transverse effects were investigated. For $n = 2$ the present model reduces to that studied in Ref.[16].

The Hamiltonian H_{drive} describes the input fields, with amplitudes α_n^{in}, entering the cavity through the fixed mirror whose partial transmission determines the input-output rate γ_c. Finally, H_{int} represents the ponderomotive interaction between the mirror and the radiation fields [23]. Such interaction is generated by the radiation pressure induced variation of the cavity length, which corresponds to a variation of the frequencies (energy levels) through Eq.(1), that is

$$\delta\,\omega_{c\,n} = \frac{\partial\,\omega_{c\,n}}{\partial\,L}\,\partial\,L = -\frac{\omega_{c\,n}}{L}\,Q \,, \tag{6}$$

with $Q = \delta L \ll L$. Since we shall consider few modes whose $\tilde{n} \ll c/(2L)$ differ not too much each other, we can set $(\omega_{c\,n}/L) \simeq G$, $\forall\, n$, as the optomechanical coupling constant.

By using Eq.(2), and accounting for the losses and the noises, we can describe the complete dynamics of the system through the following quantum Langevin equations

$$\dot{Q}(t) = \frac{P(t)}{m} \,, \tag{7}$$

$$\dot{P}(t) = -\,m\,\omega_m^2\,Q(t) + \hbar\,G \sum_n A_n^\dagger(t)\,A_n(t) - 2\,\gamma_m\,P(t) - \xi(t) \,, \tag{8}$$

$$\dot{A}_n(t) = -\,i\,(\omega_{c\,n} - \omega_{0\,n})\,A_n(t) + i\,G\,A_n(t)\,Q(t) + \sqrt{\gamma_c}\,\alpha_n^{in} - \frac{\gamma_c}{2}\,A_n(t) + \sqrt{\gamma_c}\,a_n^{in}(t) \,, \tag{9}$$

where we have used the replacements $A_n(t) \to A_n e^{-i\omega_{0\,n} t}$. Furthermore, a_n^{in} are the vacuum noise operators associated to the input radiation fields, while $\xi(t)$ is the noise operator for the quantum Brownian motion of the mirror. The noise correlations are [24, 25]

$$\langle\, a_j^{in}(t)\, a_k^{in\,\dagger}(t') \,\rangle = \delta\,(t - t')\,\delta_{j,k} \,, \tag{10}$$

$$\langle\, \xi(t)\,\xi(t') \,\rangle = \frac{m\,\gamma_m\,\hbar}{\pi} \int d\omega \left\{ \frac{\omega \left[\coth\left(\frac{\hbar\,\omega}{2\,K_B\,T} \right) - 1 \right]}{\exp\left(-\,i\,\omega\,(t - t') \right)} \right\} \,, \tag{11}$$

where k_B is the Boltzmann constant. It is worth noting that Eq.(11) gives the exact thermal noise correlations at any temperature T [25].

We are now going to study the dynamics of the small fluctuations around the steady state, i.e. the dynamics of the operators

$$q(t) = Q(t) - x\,, \tag{12}$$
$$p(t) = P(t) - y\,, \tag{13}$$
$$a_n(t) = A_n - \alpha_n\,, \tag{14}$$

where the (classical) stationary values are given by

$$x \equiv \langle Q \rangle_{ss} = \frac{\hbar G}{m\omega_m^2} \sum_n |\,\alpha_n\,|^2\,, \tag{15}$$
$$y \equiv \langle P \rangle_{ss} = 0\,, \tag{16}$$
$$\alpha_n \equiv \langle A_n \rangle_{ss} = \frac{\alpha_n^{in}}{\sqrt{\gamma_c}\,\left(\frac{1}{2} - i\,\Delta_n\right)}\,, \tag{17}$$

with

$$\Delta_n = \frac{\omega_{0\,n} - \omega_{c\,n} + G\,x}{\gamma_c}\,, \tag{18}$$

the (dimensionless) overall detuning due to the frequency mismatch and to the radiation phase shift caused by the stationary displacement x of the mirror.

For the sake of simplicity we assume, from now on, symmetric conditions for the various radiation modes, that is, $\Delta_n = \Delta$ and $\alpha_n = \alpha \in \Re$, $\forall n$. Then, it is easily recognizable in Eq.(17) the nonlinear relation between input and intracavity intensity field which give rise to the bistable behavior of the system [26].

Linearizing Eqs.(7)-(9) around the steady state (15)-(17) we obtain

$$\dot{q}(t) = \frac{p(t)}{m}\,, \tag{19}$$
$$\dot{p}(t) = -\,m\,\omega_m^2\,q(t) + \hbar\,G \sum_n \left[\,\alpha^*\,a_n(t) + \alpha\,a_n^\dagger(t)\,\right] - 2\,\gamma_m\,p(t) - \xi(t)\,, \tag{20}$$
$$\dot{a}_n(t) = \left(i\,\Delta - \frac{1}{2}\right)\gamma_c\,a_n(t) + i\,G\,\alpha\,q(t) + \sqrt{\gamma_c}\,a_n^{in}(t)\,. \tag{21}$$

Going into the frequency domain, and eliminating the mirror's variables we are left with a set of $2N$ linear equations (N being the number of driven modes, so that $n = 1, \ldots, N$) for the modes quadratures

$$X_n(\omega) = \frac{a_n(\omega) + a_n^\dagger(-\omega)}{\sqrt{2}}\,, \tag{22}$$
$$Y_n(\omega) = -\,i\,\frac{a_n(\omega) - a_n^\dagger(-\omega)}{\sqrt{2}}\,. \tag{23}$$

Such equations can be written in compact form as

$$i\,\omega\,\mathbf{v}(\omega) = \mathcal{M}(\omega)\,\mathbf{v}(\omega) + \sqrt{\gamma_c}\,\mathbf{v}^{\,in}(\omega) + \mathbf{s}(\omega)\,\xi(\omega)\,, \tag{24}$$

where we have introduced the $2N$ dimensional vectors

$$\mathbf{v}(\omega) = (X_1(\omega), Y_1(\omega), \ldots, X_N(\omega), Y_N(\omega))^T, \tag{25}$$

$$\mathbf{v}^{in}(\omega) = \left(X_1^{in}(\omega), Y_1^{in}(\omega), \ldots, X_N^{in}(\omega), Y_N^{in}(\omega)\right)^T, \tag{26}$$

$$\mathbf{s}(\omega) = \sqrt{2}\, G\, \chi(\omega)\, (0, -\alpha, \ldots 0, -\alpha)^T, \tag{27}$$

with

$$\chi(\omega) = \frac{1}{m\,(\omega_m^2 - \omega^2 + 2\,i\,\gamma_m\,\omega)}, \tag{28}$$

the mirror's mechanical response function. Furthermore, $\mathcal{M}(\omega)$ is a $2N \times 2N$ matrix written as

$$\mathcal{M} = \begin{pmatrix} \mathcal{M}_d & \mathcal{M}_o & \cdots & \mathcal{M}_o \\ \mathcal{M}_o & \mathcal{M}_d & \cdots & \mathcal{M}_o \\ \vdots & \vdots & \ddots & \vdots \\ \mathcal{M}_o & \mathcal{M}_o & \cdots & \mathcal{M}_d \end{pmatrix}, \tag{29}$$

where $\mathcal{M}_d$ and $\mathcal{M}_o$ are 2×2 matrices given by

$$\mathcal{M}_d = \begin{pmatrix} -\gamma_c/2 & -\Delta\gamma_c \\ \Delta\gamma_c + 2\hbar G^2 \chi(\omega)\alpha^2 & -\gamma_c/2 \end{pmatrix}, \tag{30}$$

$$\mathcal{M}_o = \begin{pmatrix} 0 & 0 \\ 2\hbar G^2 \chi(\omega)\alpha^2 & 0 \end{pmatrix}. \tag{31}$$

The useful noise correlations for Eq.(24) come from Eqs.(10),(11),(22),(23) and read

$$\left\langle X_j^{in}(\omega)\, X_k^{in}(\omega') \right\rangle = \frac{1}{2}\,\delta_{j,k}\,\delta(\omega + \omega'), \tag{32}$$

$$\left\langle Y_j^{in}(\omega)\, Y_k^{in}(\omega') \right\rangle = \frac{1}{2}\,\delta_{j,k}\,\delta(\omega + \omega'), \tag{33}$$

$$\left\langle X_j^{in}(\omega)\, Y_k^{in}(\omega') \right\rangle = \frac{1}{2}\,i\,\delta_{j,k}\,\delta(\omega + \omega'), \tag{34}$$

and

$$\langle \xi(\omega)\, \xi(\omega') \rangle = \left\{ 1 + \coth\left(\frac{\hbar\,\omega}{2\,K_B\,T} \right) \right\} \frac{m\,\gamma_m\,\hbar}{\pi}\,\omega\,\delta(\omega + \omega'). \tag{35}$$

Thus Eqs.(24)-(35) completely describe the dynamics of the small fluctuations of radiation modes. Practically, we can see from Eqs.(39),(40) that the mirror mediates information between the radiation modes leading to an effective mode-mode interaction as results from Eqs.(24), (29) and (30) (31).

3. Output fields entanglement

The above discussed mode-mode interaction will presumably lead to entanglement between intracavity modes, which, in turn, should be reflected on the fields outgoing the cavity. On the other hand, only these latter become really useful. Hence, we are going to characterize their correlations. First of all we notice, by the the input-output theory [24], that

$$\mathbf{v}^{out}(\omega) = \sqrt{\gamma_c}\,\mathbf{v}(\omega) - \mathbf{v}^{in}(\omega), \tag{36}$$

then, we introduce the hermitian output quadrature operators

$$\begin{aligned} R_{X_n^{out}} &= \frac{X_n^{out}(\omega) + X_n^{out}(-\omega)}{2}, \\ R_{Y_n^{out}} &= \frac{Y_n^{out}(\omega) + Y_n^{out}(-\omega)}{2}. \end{aligned} \tag{37}$$

Their correlations are described by the $2N \times 2N$ matrix

$$\begin{aligned} \mathcal{G} &\equiv \frac{1}{4} \langle \mathbf{v}^{out}(\omega) \left[\mathbf{v}^{out}(-\omega)\right]^T + \mathbf{v}^{out}(-\omega) \left[\mathbf{v}^{out}(\omega)\right]^T \rangle, \\ &= \frac{1}{4} \mathcal{K}(\omega) \langle \mathbf{v}^{in}(\omega) \left[\mathbf{v}^{in}(-\omega)\right]^T \rangle \left[\mathcal{K}(-\omega)\right]^T \\ &+ \frac{1}{4} \mathcal{K}(-\omega) \langle \mathbf{v}^{in}(-\omega) \left[\mathbf{v}^{in}(\omega)\right]^T \rangle \left[\mathcal{K}(\omega)\right]^T \\ &+ \frac{\gamma_c}{4} \mathcal{L}^{-1}(\omega) \mathbf{s}(\omega) \left[\mathbf{s}(-\omega)\right]^T \left[\mathcal{L}^{-1}(-\omega)\right]^T \langle \xi(\omega) \xi(-\omega) \rangle \\ &+ \frac{\gamma_c}{4} \mathcal{L}^{-1}(-\omega) \mathbf{s}(-\omega) \left[\mathbf{s}(\omega)\right]^T \left[\mathcal{L}^{-1}(\omega)\right]^T \langle \xi(-\omega) \xi(\omega) \rangle, \end{aligned} \tag{38}$$

where

$$\mathcal{K}(\omega) = \gamma_c \mathcal{L}^{-1}(\omega) - \mathcal{I}, \tag{39}$$

$$\mathcal{L}(\omega) = i\omega\mathcal{I} - \mathcal{M}(\omega), \tag{40}$$

with $\mathcal{I}$ the identity $2N \times 2N$ matrix.

By virtue of the linearization procedure adopted in Sec.II we have in output, for each frequency, a multivariate Gaussian state. Such states can be described by a Wigner function with a frequency dependent symmetric correlation matrix. However, the matrix $\mathcal{G}$ is not symmetric and, moreover, it concerns quadratures with frequency dependent commutator, i.e.,

$$\langle \left[R_{X_n^{out}}(\omega), R_{Y_n^{out}}(-\omega) \right] \rangle = i\, c(\omega), \quad \forall n, \tag{41}$$

with c a real positive definite function of frequency ω, i.e. $ic(\omega) = \mathcal{G}_{2n-1,2n}(\omega) - \mathcal{G}_{2n,2n-1}(\omega)$ for $n = 1, \ldots N$. Then, since the entanglement criteria [19, 16, 18] are formulated in terms of quadratures with canonical commutation relations, i.e., $[R_X, R_Y] = i$, we construct from Eqs.(38), (41) a symmetric correlation matrix concerning such type of quadratures, that is

$$\mathcal{V}_{j,k}(\omega) = \frac{\mathcal{G}_{j,k}(\omega) + \mathcal{G}_{k,j}(\omega)}{2c(\omega)}. \tag{42}$$

We henceforth consider multivariate Gaussian states completely characterized by Eq.(42).

3.1. *Bipartite entanglement*

We now restrict the attention to only two mode ($N = 2$) in order to study the entanglement of a bipartite system. Practically we consider

$$\mathcal{M} = \begin{pmatrix} \mathcal{M}_d & \mathcal{M}_o \\ \mathcal{M}_o & \mathcal{M}_d \end{pmatrix}, \tag{43}$$

Table 1. Parameters values.

ω_m	10^6 s^{-1}
$\omega_{0\,n}$	10^{15} s^{-1}
m	10^{-4} kg
L	10^{-3} m
γ_m	1 s^{-1}
γ_c	10^6 s^{-1}
$P_n^{in} = \hbar\omega_{0\,n}\|\alpha_n^{in}\|^2$	13 mW per mode

and we introduce the matrices

$$\mathcal{J} = \begin{pmatrix} 0 & 1 \\ -1 & 0 \end{pmatrix}, \qquad \mathcal{R} = \begin{pmatrix} 1 & 0 \\ 0 & -1 \end{pmatrix}. \tag{44}$$

Then, Eq.(43) leads to

$$\mathcal{V} = \begin{pmatrix} \mathcal{A} & \mathcal{C} \\ \mathcal{C}^T & \mathcal{A} \end{pmatrix}, \tag{45}$$

where $\mathcal{A}$ and $\mathcal{C}$ are 2×2 matrices. In this case the Simon's criterion [19] is necessary and sufficient for entanglement, and, according to Eq.(19) of Ref.[19] we can define a marker of entanglement as

$$E = 1 + (\det\mathcal{A})^2 + \left(\frac{1}{4} - |\det\mathcal{C}|\right)^2 - \mathrm{tr}\left\{\mathcal{A}\mathcal{J}\mathcal{C}\mathcal{J}\mathcal{A}\mathcal{J}\mathcal{C}^T\mathcal{J}\right\} - \frac{1}{2}\det\mathcal{A}\,, \tag{46}$$

so that, if it goes below 1, the state is entangled. Instead, the product criterion introduced in Ref.[8], and reminiscent of nonlocality criterion [27], gives

$$E = 4(\mathcal{A}_{11} + \mathcal{C}_{11})(\mathcal{A}_{22} - \mathcal{C}_{22})\,. \tag{47}$$

Finally, the sum criterion, expressed by Eq.(3) of Ref.[18], can be rewritten as

$$E = \mathrm{tr}\{\mathcal{A}\} + \mathrm{tr}\,\{\mathcal{C}\mathcal{R}\}\,. \tag{48}$$

Then, in Fig.2 we report the marker of entanglement E versus ω, for the three criteria a) Simon, b) product, c) sum. At any given frequency ω, E is calculated from the corresponding output quadrature correlations. The latter can be detected, for instance, by two separate homodyne receivers having the same (fixed) analysis frequency ω (see Ref.[28]).

The parameters values of Fig.2 are taken similar to those of the experimental set up of Ref.[10]. They are written in Tab.I. Fig.2 shows that in case of no detuning the product and the sum criteria do not reveal any entanglement, while the Simon criterion does. This proves the weakness of the the entanglement coming in this case from the interaction of only amplitude quadratures as can be evicted from Eqs.(43) and (30),(31). Such type of entanglement, although resistant to thermal effects, is practically useless in information processing like teleportation whose performance are much more related to the product and sum criteria [29].

As stated above, the Simon's criterion, being necessary and sufficient in our case, recognizes all the possible entangled states. In this sense it is weaker than the other criteria. Since we are

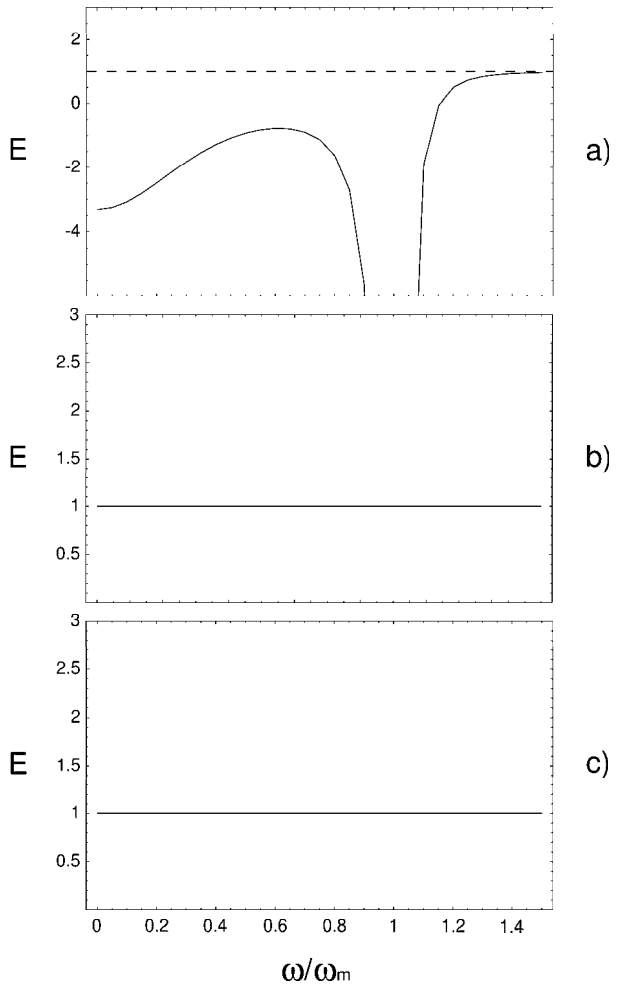

Fig. 2. The marker of entanglement E is plotted versus ω with respect to the three criteria a) Simon, b) product, c) sum. Here $\Delta = 0$ and the other parameter values are given in Tab.I. The dashed lines indicate the limiting value below which entanglement is recognized. The three plots remain unalterated in the temperature range $T = 0 \div 300$ K.

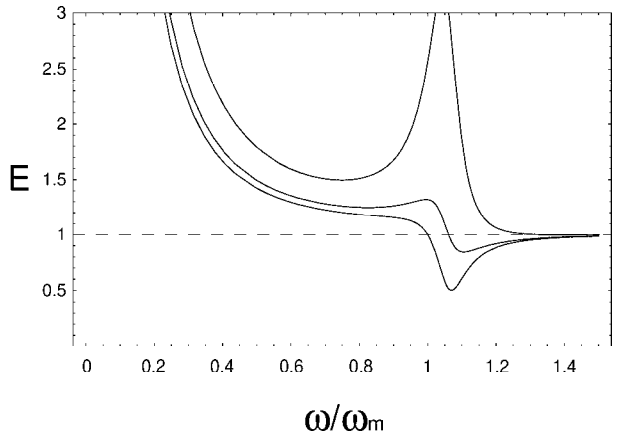

Fig. 3. The entanglement indicator E of Eq.(48) is plotted versus ω. Here $\Delta = -0.1$, and solid lines are for $T = 0$, $T = 10$, $T = 50$ K from botton to top. The other parameter values are given in Tab.I. The dashed line indicates the limiting value below which entanglement is recognized.

interested on possible applications requiring strong enough entanglement, we leave the Simon's criterion aside. Due also to the fact that the sum criterion always implies the product one [30] we henceforth consider only the sum criterion. Then in Figs.3 and 4 we have shown the beneficial effect of the detuning on the entanglement. As matter of fact it allows interaction of both amplitude and phase quadratures as can be seen in Eq.(43). In particular Fig.4 exhibits the presence of entanglement at low frequencies (according to Ref.[16]) as well as near the mechanical resonance. Neverthless, the latter turns out to be more sensible to the thermal noise. This behavior resembles that of the light squeezing studied in Refs.[4, 5].

3.2. *Tripartite entanglement*

Characterization of multipartite entanglement ($N > 2$) is a more complex issue [14]. In general, multi-party inseparability criteria cannot be formulated in compact form as for the two-party. Here, we consider $N = 3$, thus the matrix

$$\mathcal{M} = \begin{pmatrix} \mathcal{M}_d & \mathcal{M}_o & \mathcal{M}_o \\ \mathcal{M}_o & \mathcal{M}_d & \mathcal{M}_o \\ \mathcal{M}_o & \mathcal{M}_o & \mathcal{M}_d \end{pmatrix}, \tag{49}$$

which leads to

$$\mathcal{V} = \begin{pmatrix} \mathcal{A} & \mathcal{C} & \mathcal{C} \\ \mathcal{C}^T & \mathcal{A} & \mathcal{C} \\ \mathcal{C}^T & \mathcal{C}^T & \mathcal{A} \end{pmatrix}. \tag{50}$$

Although for three-mode Gaussian states there exist a necessary and sufficient separability criterion [31], its violation does not necessarily witness genuine tripartite entanglement. However, from the symmetry of matrix (50) we easily deduce that the conditions for bipartite entanglement also give tripartite entanglement. As matter of fact a tripartite fully inseparable state is that which cannot be separate for any grouping of the parties [31]. But, due to the

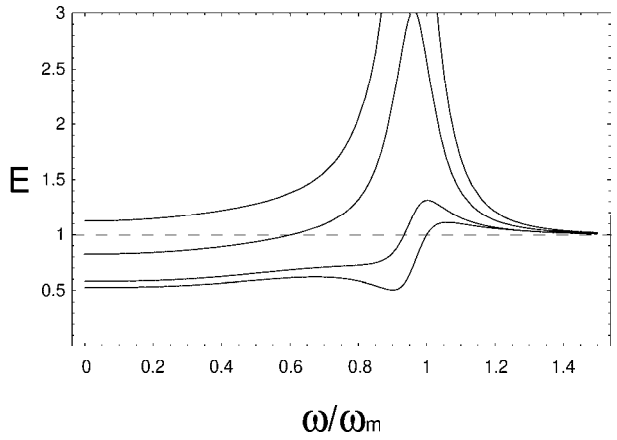

Fig. 4. The entanglement indicator E of Eq.(48) is plotted versus ω. Here $\Delta = 0.1$, and solit lines are for $T = 0$, $T = 10$, $T = 50$, $T = 100$ K from botton to top. The other parameter values are given in Tab.I. The dashed line indicates the limiting value below which entanglement is recognized.

symmetry among the parties, if two of them show entanglement according to Sec. III A, then any two of them show entanglement, thus revealing a fully inseparable state.

4. Applications to remote state transfer

This ponderomotive entanglement find possible applications in quantum information processings with continuous variables [14]. Here, we deal with the possibility of using it for remote state transfer. By referring to Fig.1, the modes outgoing the cavity can be separated and one of them can reach a sending station while the others reach receiving stations. Then, all these modes constitute the quantum channel to exploit for transferring a quantum state from the sending station to the receiving ones. We will analyze in detail the case for $N = 2$, i.e., teleportation [20, 21], and $N = 3$, i.e., telecloning [22].

4.1. *Teleportation*

The standard teleportation protocol for continuous variable [20, 21] can be described by a convolution of the Wigner functions [32]

$$W_r(\beta) = \int d^2\xi \, W_s(\xi) \, K(\beta - \xi) \,, \tag{51}$$

$$K(\beta - \xi) = \int d^2\xi' \, W(\xi'^* - \xi^* \,, \beta - \xi') \,, \tag{52}$$

where W_r is the Wigner function of the received state, W_s that of the unknown state to be transferred (sent), and W that describing the quantum channel between the two stations, i.e., the two entangled modes characterized by the correlation matrix (45). Here, small greek letters are for complex variables.

By Fourier transforming Eqs.(52), we get a simple relation for the characteristic functions

Φ, namely

$$\Phi_r(\lambda) \,=\, \Phi_s(\lambda)\,\tilde{K}(\lambda)\,, \tag{53}$$

where

$$\begin{aligned}\tilde{K}(\lambda) \;&\equiv\; \int d^2\kappa\, K(\kappa)\, \exp(-i\kappa_1\lambda_1 - i\kappa_2\lambda_2) \\ &=\; \int d^2\kappa\, d^2\mu\, d^4\mathbf{z}\; \Phi(\mathbf{z}\,)\, \exp\left(-i\kappa_1\lambda_1 - i\kappa_2\lambda_2\right) \\ &\times\; \exp\left\{i\,\mathbf{z}\cdot(\mu_1, -\mu_2, \kappa_1-\mu_1, \kappa_2-\mu_2)\right\}\,,\end{aligned} \tag{54}$$

where the variables with the subscript 1 (2) represent the real (imaginary) part of the corresponding complex variables, and $\mathbf{z}$ is a four dimensional real variables vector. Moreover,

$$\Phi(\mathbf{z}\,) \,=\, \exp\left\{-\frac{1}{4}\,\mathbf{z}\;\mathcal{V}\,\mathbf{z}^T\right\}\,, \tag{55}$$

is the characteristic function describing the two-mode channel, thus characterized by the matrix $\mathcal{V}$ given in Eq.(45).

We also consider a Gaussian state to be transferred, so that

$$\Phi_s(\lambda) \,=\, \exp\left[-\frac{1}{4}\;(\lambda_1,\lambda_2)\;\mathcal{D}\;(\lambda_1,\lambda_2)^T\right]\,, \tag{56}$$

with $\mathcal{D}$ the 2×2 correlation matrix.

Finally, the fidelity of the protocol, resulting from the overlap between the "r" and the "s" Wigner functions, can be written in terms of characteristic functions as

$$F \,\equiv\, \frac{1}{4\,\pi}\int d^2\lambda\;\Phi_s(\lambda)\,\Phi_r^*(\lambda)\,. \tag{57}$$

Then, by using Eqs.(53)-(56), we arrive at (see also [33])

$$\begin{aligned}F \;&=\; \frac{1}{4\,\pi}\int d^2\lambda\, \exp\left[-\frac{1}{2}\,(\lambda_1,\lambda_2)\,\mathcal{D}\,(\lambda_1,\lambda_2)^T\right] \\ &\times\; \exp\left[-\frac{1}{4}\,(\lambda_1,-\lambda_2,\lambda_1,\lambda_2)\,\mathcal{V}\,(\lambda_1,-\lambda_2,\lambda_1,\lambda_2)^T\right] \\ &=\; \frac{1}{\sqrt{\det\left(2\mathcal{D}+\mathcal{R}^T\mathcal{A}\mathcal{R}+\mathcal{R}^T\mathcal{C}+\mathcal{C}^T\mathcal{R}+\mathcal{A}\right)}}\,.\end{aligned} \tag{58}$$

In Fig.5 we show the teleportation fidelity as function of ω. As a state to be teleported we have chosen the coherent state for which $\mathcal{D} = \mathrm{diag}(1/2, 1/2)$. In such a case the upper bound for the fidelity achievable with only classical means and no quantum resources is $1/2$ [29]. Then, we see that this bound is overcame just in correspondence of the minima of Fig.3. Also the behavior of the fidelity in terms of thermal noise reflects that of the entanglement recognized by the sum criterion (see Fig.4). Instead this behavior is not strictly related to the Simon's criterion [29].

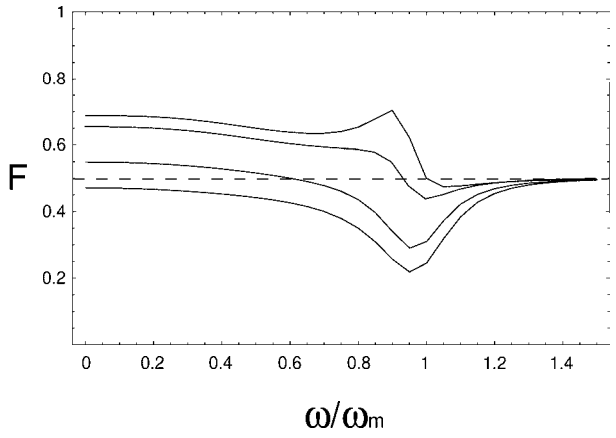

Fig. 5. Teleportation fidelity versus ω. Curves from top to bottom are for $T = 0$, $T = 10$, $T = 50$, $T = 100$ K. Here $\Delta = 0.1$ and the values of other parameters listed in Tab.I. The dashed line indicates the classical upper bound.

4.2. *Telecloning*

As a simple extension of the arguments used for teleportation, we can write the Wigner function of the received state (at the two stations) by the convolution [22]

$$\breve{W}_r(\beta,\eta) = \int d^2\xi\, W_s(\xi)\, \breve{K}(\beta-\xi,\eta-\xi)\,, \tag{59}$$

$$\breve{K}(\beta-\xi,\eta-\xi) = \int d^2\xi'\, W(\xi'^{*}-\xi^{*}\,,\,\beta-\xi'\,,\,\eta-\xi')\,, \tag{60}$$

where W is the Wigner function describing the quantum channel between sending and receiving stations, i.e. the three entangled modes characterized by the correlation matrix (50).

The state at one receiving station can be obtained by tracing the received state (59) over the other receiving station. Due to the symmetry, the two possible states coming out coincide. Thus, we can assume

$$W_r\,(\beta) = \int d^2\eta\, \breve{W}_r(\beta,\eta) = \int d^2\xi W_s(\xi) K(\beta-\xi)\,, \tag{61}$$

where now

$$K(\beta-\xi) = \int d^2\eta\, \breve{K}(\beta-\xi,\eta-\xi)\,. \tag{62}$$

By again Fourier transforming Eq.(61), we end up with a relation for the characteristic functions identical to Eq.(53),

$$\Phi_r(\lambda) = \Phi_s(\lambda)\, \tilde{K}(\lambda)\,, \tag{63}$$

where now

$$\begin{aligned}\tilde{K}(\lambda) &= \int d^2\kappa\, \exp\left(-i\kappa_1\lambda_1 - i\kappa_2\lambda_2\right) \\ &\times \int d^2\mu\, d^2\zeta\, d^6\mathbf{z}\, \Phi(\mathbf{z})\, \exp\left\{i\mathbf{z}\cdot(\mu_1,-\mu_2,\kappa_1-\mu_1,\kappa_2-\mu_2,\zeta_1-\mu_1,\zeta_2-\mu_2)^T\right\}\end{aligned} \tag{64}$$

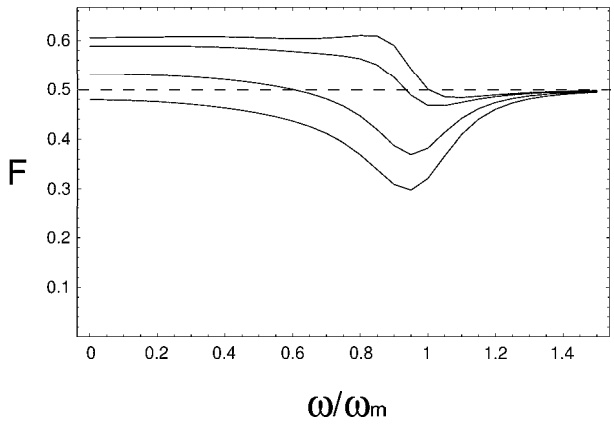

Fig. 6. Telecloning fidelity versus ω. Curves from top to bottom are for $T = 0$, $T = 10$, $T = 50$, $T = 100$ K. Here $\Delta = 0.1$ and the values of other parameters listed in Tab.I. The dashed line indicates the classical upper bound.

and

$$\Phi(\mathbf{z}) = \exp\left[-\frac{1}{4}\,\mathbf{z}\,\mathcal{V}\,\mathbf{z}^T\right], \tag{65}$$

is the characteristic function describing the three-mode channel, thus characterized by the matrix $\mathcal{V}$ given in Eq.(50), with $\mathbf{z}$ a 6 dimensional real variables vector.

We again consider a Gaussian state to be transferred, as in Eq.(56). Then, the fidelity, being expressed by Eq.(57), results, by means of Eqs. (56), (63), (64), (65) as

$$\begin{aligned} F &= \frac{1}{4\,\pi}\int d^2\lambda\,\exp\left[-\frac{1}{2}\,(\lambda_1,\lambda_2)\,\mathcal{D}\,(\lambda_1,\lambda_2)^T\right] \\ &\times \exp\left[-\frac{1}{4}\,(\lambda_1,-\lambda_2,\lambda_1,\lambda_2,0,0)\,\mathcal{V}\,(\lambda_1,-\lambda_2,\lambda_1,\lambda_2,0,0)^T\right] \\ &= \frac{1}{\sqrt{\det\left(2\mathcal{D}+\mathcal{R}^T\mathcal{A}\mathcal{R}+\mathcal{R}^T\mathcal{C}+\mathcal{C}^T\mathcal{R}+\mathcal{A}\right)}}\,. \end{aligned} \tag{66}$$

It practically coincides with Eq.(58). However, in this case, F is limited above by $2/3$ [34], due to the no-cloning theorem [35].

In Fig.6 we show the telecloning fidelity as function of ω. As state to be telecloned we have choosen again a coherent state for which $\mathcal{D} = \mathrm{diag}(1/2, 1/2)$. Also in this case the upper classical bound for the fidelity is $1/2$ [34]. Then, we see that this bound is overcome again in correspondence of the minima of Fig.4 confirming the arguments at the end of the previous subsection.

5. Conclusions

In conclusion, we have studied *ponderomotive entanglement*, that is entanglement between radiation modes generated by the radiation pressure effects. In doing so we have also provided a comparison between different entanglement criteria. Practically, we have shown that even a classical force, like radiation pressure force, together with macroscopic objects can be used for

quantum information purposes. This is novel and unexpected result, as quantum information is usually recognized to be very fragile. We have further investigated the role played by the thermal noise related to the mechanical motion of the mirror. We have seen that purely quantum effects can survive up to a temperature ≈ 10 K. This is within reach in experiments with really macroscopic mirrors [10]. Thus, the present study has a fundational interest for better understanding the tricky borderline between classical and quantum worlds (see also [7]). Quantum teleportation is, indeed, thought to be degraded to the classical limit by only one thermal phonon [18]. Instead, we have shown that this transition strongly depends on the way the noise comes into the system. Moreover, an experimental evidence of the cross-over between quantum and classical regime in terms of information aspects seems at the hands by just varying the bath temperature.

From an applicative point of view, our model could be suitable as well for micro-opto-mechanical-systems (MOMS) [36] used for quantum information purposes. These could become alternative to other systems for producing entangled states for continuous variables. In fact, such systems usually work at mechanical frequencies higher than the macroscopic mirrors (up to GHz) and they allow to reach lower temperatures (down to few mK), assuring better performances. On the other hand, the fidelity in remote state transfer we have shown, although overcome the classical bounds, does not reach the optimal values. Theoretically, these could be obtained by an optimization of all involved parameters. Also the local operations could be optimized for the studied type of Gaussian entangled channel [33]. However, all that would require large numerical resources without adding new physics to the problem. So it has been left apart by only providing a qualitative study of ponderomotive entanglement.

References

1. V. B. Braginsky and F. Y. Khalili, *Quantum Measurement*, (Cambridge University Press, Cambridge, 1992).
2. A. Abramovici, *et al.*, Science **256**, 325 (1992).
3. D. Rugar and P. Hansma, Phys. Today **43**(10), 23 (1990).
4. C. Fabre, M. Pinard, S. Bourzeix, A. Heidmann, E. Giacobino and S. Reynaud, Phys. Rev. A **49**, 1337 (1994).
5. S. Mancini and P. Tombesi, Phys. Rev. A **49**, 4055 (1994).
6. S. Mancini, V. I. Man'ko and P. Tombesi, Phys. Rev. A **55**, 3042 (1997); S. Bose, K. Jacobs and P. L. Knight, Phys. Rev. A **56**, 4175 (1997).
7. S. Bose, K. Jacobs and P. L. Knight, Phys. Rev. A **59**, 3204 (1999); W. Marshall, C. Simon, R. Penrose and D. Bouwmeester, arXiv:quant-ph/0210001.
8. S. Mancini, V. Giovannetti, D. Vitali and P. Tombesi, Phys. Rev. Lett. **88**, 120401 (2002).
9. I. Tittonen, T. Kalkbrenner, G. Breitenbach, T. Muller, R. Conradt, S. Schiller, E. Steinsland, N. Blanc and N. F. de Rooij, Phys. Rev. A **59**, 1038 (1999).
10. P. F. Cohadon, A. Heidmann, and M. Pinard, Phys. Rev. Lett. **83**, 3174 (1999); Y. Hadjar, P. Cohadon, C. G. Aminoff, M. Pinard and A. Heidmann, Europhys. Lett. **46**, 545 (1999); T. Briant, P. F. Cohadon, M. Pinard and A. Heidmann, Eur. Phys. J. D **22**, 121 (2003).
11. C. H. Bennett and D. P. DiVincenzo, Nature(London) **404**, 247 (2000).
12. E. Schrödinger, Naturwissenschaften **23**, 807 (1935); *ibid.* **23**, 823 (1935); *ibid.* **23**, 844 (1935).
13. A. Einstein, B. Podolsky, and N. Rosen, Phys Rev. **47**, 777 (1935).
14. S. L. Braunstein and A. K. Pati, *Quantum Information Theory with Continuous Variables*, (Kluwer Academic Publishers, Dodrecht, 2001).
15. S. Mancini, Phys. Lett. A **279**, 1 (2001).

16. V. Giovannetti, S. Mancini and P. Tombesi, Europhys. Lett. **54**, 559 (2001).
17. S. Mancini and A. Gatti, J. Opt. B: Quantum and Semiclass. Opt. **3**, S66 (2001).
18. L. M. Duan, G. Giedke, J. I. Cirac and P. Zoller, Phys. Rev. Lett. **84**, 2722 (2000).
19. R. Simon, Phys. Rev. Lett. **84**, 2726 (2000).
20. L. Vaidman, Phys. Rev. A **49**, 1473 (1994).
21. S. L. Braunstein and H. J. Kimble, Phys. Rev. Lett. **80**, 869 (1998).
22. P. van Loock and S. L. Braunstein, Phys. Rev. Lett. **87**, 247901 (2001).
23. C. K. Law, Phys. Rev. A **51**, 2537 (1995).
24. C. W. Gardiner, *Quantum Noise* (Springer, Heidelberg, 1991).
25. V. Giovannetti and D. Vitali, Phys. Rev. A, **63** 023812 (2001).
26. A. Dorsel, J. C. McCullen, P. Meystre, E. Vignes and H. Walther, Phys. Rev. Lett. **51**, 1550 (1983); A. Gozzini, F. Maccarone, F. Mango, I. Longo and S. Barbarino, J. Opt. Soc. Am. B **2**, 1841 (1985).
27. M. D. Reid, Phys. Rev. A **40**, 913 (1989).
28. Z. Y. Ou, S. F. Pereira, H. J. Kimble and K. C. Peng, Phys. Rev. Lett. **68**, 3663 (1992).
29. S. L. Braunstein, C. Fuchs, H. J. Kimble, P. van Loock, Phys. Rev. A **64**, 022321 (2001).
30. V. Giovannetti, S. Mancini, D. Vitali and P. Tombesi, Phys. Rev. A **67**, 022320 (2003).
31. G. Giedke, B. Kraus, M. Lewenstein and J. I. Cirac, Phys. Rev. A **64**, 052303 (2001).
32. A. V. Chizhov, L. Knöll and D. G. Welsch, Phys. Rev. A **65**, 022310 (2002).
33. J. Fiurášek, Phys. Rev. A **66**, 012304 (2002).
34. N. J. Cerf and S. Iblisdir, Phys. Rev. A **62**, 040301 (2000).
35. W. K. Wooters and W. H. Zurek, Nature(London) **299**, 802 (1982).
36. T. D. Stowe, K. Yasumura, T. W. Kenny, D. Botkin, K. Wago and D. Rugar, Appl. Phys. Lett. **71**, 288 (1997); A. N. Cleland and M. L. Roukes, Nature(London) **392**, 160 (1998); H. J. Mamin and D. Rugar, Appl. Phys. Lett. **79**, 3358 (2001).